NUMERICAL SIMULATION OF NANOFLUID INJECTION IN OIL SATURATED POROUS MEDIA WITH ENVIRONMENTAL APPLICATIONS

Alexandra Sikinioti-Lock, Katerina Terzi, Maria Theodoropoulou, Christos Tsakiroglou
Foundation for Research and Technology Hellas – Institute of Chemical Engineering Sciences, Stadiou str., Platani, 26504 Patras, Greece

This paper was prepared for presentation at the International Symposium of the Society of Core Analysts held in Trondheim, Norway, 27-30 August 2018

ABSTRACT

A macroscopic numerical model is developed to simulate the flow, mass-transfer, and reactive processes when a suspension of zero-valent iron nanoparticles (nZVI) is injected in a porous medium, polluted by a chlorinated non-aqueous phase liquid (NAPL) at its residual saturation. The nanoparticles transport is coupled with their non-equilibrium deposition in a porous medium, and the parameters quantifying the kinetics of nanoparticle attachment / detachment in sand grains are estimated with inverse modeling of experimental results from nZVI flow tests in a sand column. The kinetics of the reaction of nZVI with dissolved tetrachloroethylene (PCE) is based on the numerical predictions of the statistical shrinking-core model that couples the mass-transfer with reactive processes at the nanoparticle scale. Then, the NP transport model is extended to reactive flows by combining the dynamics of PCE ganglia dissolution and nZVI reactions with mass balances for residual PCE saturation, dissolved PCE concentration, and nZVI concentration in aqueous phase. Numerical predictions of the residual PCE remediation efficiency as a function of injected NP mass is compared with experimental results of a PCE source zone remediation test performed in a sand column. The PCE source zone remediation efficiency is maximized, as the injected nZVI maintains its reactivity for a long period of time, and along the longest length of the porous medium. If updated to 3-D media, and accounting for the real hydrogeology and contaminant reaction kinetics, the simulator might be used as a tool to predict the spatial and temporal evolution of the NAPL source zone during the in situ nano-remediation of heavily contaminated aquifers.

INTRODUCTION

Among the various materials explored for nano-remediation, the nanoscale zero-valent iron (nZVI) is currently the most widely used for the in situ remediation of aquifers from a variety of toxic pollutants (e.g. reduction of chlorinated hydrocarbons, and nitro-aromatics, sorption/geochemical trapping of heavy metals/metalloids) (Mueller et al., 2012). Thus far, from continuum viewpoint, there is a limited number of comprehensive reviews focusing on all the possible transport mechanisms of NP in porous media and their superposition within the context of continuum modeling. These mechanisms comprise reversible, irreversible and equilibrium interactions of NP with porous media,

as well as agglomeration, straining, blocking, ripening, and size exclusion (Molnar al., 2015; Babakhani et al., 2017).
Recently, Tosco and her collaborators (Tosco and Sethi, 2010; Tosco et al., 2014) have developed a multi-parameter continuum model of nano-colloid flow and transport in porous media and used it for interpreting lab-scale tests of increasing complexity. It should be mentioned that the main drawback of such complex models is the increasing uncertainty of parameter values estimated with inverse modeling. Regarding the numerical modeling of PCE ganglia remediation in soils, attention was paid on the investigation of systems where high nZVI concentration suspensions are injected, and only the nZVI immobilized on sand grains is reactive (Taghavy et al., 2010; Fagerlund et al., 2012).
In the present work, based on the model of Tosco et al. (2014), first, a macroscopic numerical model of nZVI flow through a porous medium is developed. With inverse modeling of the iron concentration breakthrough curves of a sandpack, the parameters describing the kinetics of nanoparticle attachment / detachment are estimated. Then, the macroscopic model is extended to reactive flows with mass balances describing the dynamics of non-aqueous phase liquid (NAPL) dissolution, dissolved pollutant and PCE ganglia reaction with suspended nZVI, and the subsequent decrease of the saturation of the NAPL source zone. To quantify the kinetics of dissolved pollutant (PCE) reaction with nZVI, the numerical predictions of a statistical shrinking core model (Tsakiroglou et al., 2017) are fitted to appropriate kinetic models. The simulator is assessed with respect to its capability to predict results from NAPL (PCE source zone) remediation test in a sand column.

METHODS AND MATERIALS

3.1 Experiments in porous media

Aqueous suspensions of carboxyl-methyl-cellulose (CMC)-coated nZVI were prepared at concentration ~ 1 g/L, by the sodium borohydrite method, and detailed information is reported elsewhere (Tsakiroglou et al., 2016). nZVI flow and PCE remediation experiments were performed in a column (L=31cm, D=3cm) packed with a commercial silicate sand (grain zizes~100-450μm, d_{50}=375 μm, ε_0=0.44, k_0=86 D). The sand column was evacuated, filled with distilled and degassed water (DDW), and the aqueous suspension of CMC-coated nZVI was injected for 7.5 hrs under a constant influx rate 1 mL/min, and then was flushed with DDW for 5 hrs under the same influx rate. Samples collected from column effluent with an automatic fractional collector, were digested with HNO_3 to measure the iron concentration with atomic absorption spectroscopy (AAS). At the end of experiment, the sand column was sliced into 14 segments, samples were removed from each segment and mixed with HNO_3 solution to dissolve the iron. The solution was filtered and the residual iron was measured with AAS. In the same sandpack, an experiment of the in situ remediation of PCE source zone (residual PCE) was performed. Initially the sand column was evacuated and saturated completely with PCE, 2 Pore Volumes (PVs; 1 PV=103 mL) of DDW were injected at flow rate 3 mL/min., and the residual PCE saturation at the end of primary imbibition was

determined with a mass balance based on the different densities of the two fluids. Then, 1 PV of DDW was injected at flow rate 1 mL/min, followed by the injection of 3.3 PVs of CMC-coated nZVI suspension at the same flow rate. To determine the PCE concentration in effluent, the PCE was extracted with n-hexane from samples collected in a fractional collector, and the extracts were centrifuged, filtered and analyzed with gas chromatography – electron capacitance detector (GC-ECD). To calculate the final PCE saturation, remaining in the pore space at the end of nZVI injection, the column was flushed with 3 PVs of n-hexane to dissolve completely the PCE, and the concentration of PCE dissolved in n-hexane was measured with GC-ECD.

3.2 Model of nanoparticle (NP) transport in porous media

We assume that a suspension of nanoparticles (NPs) is injected at volumetric flow rate Q through a porous medium of length L and cross-sectional area A_t. The 1-dimensional flow of NPs is described by the mass balance

$$\frac{\partial\left(\varepsilon_m C_{NP}\right)}{\partial t}+\frac{\partial\left(\rho_b s\right)}{\partial t}=-\frac{\partial\left(u_d C_{NP}\right)}{\partial x}+\frac{\partial}{\partial x}\left(\varepsilon_m D_{L,NP}\frac{\partial C_{NP}}{\partial x}\right) \tag{1}$$

where ε_m is the porosity, C_{NP} is the nanoparticle mass concentration in suspension (kg/m^3), s is the concentration of particles deposited in the porous medium (it is defined equal to the mass of attached particles per unit mass of the porous medium), ρ_b is the initial bulk density of the porous medium, u_d ($=Q/A_t$) is the superficial (Darcy) flow velocity, and $D_{L,NP}$ is the NP longitudinal dispersion coefficient. The concentration of deposited particles, s, is regarded as the superposition of two concentrations (Bradford et al., 2009), namely

$$s = s_1 + s_2 \tag{2}$$

where, s_1 is the concentration of deposited particles due to ripening and blocking processes, described by the phenomenological model (Tosco and Sethi, 2010)

$$\frac{\partial\left(\rho_b s_1\right)}{\partial t}=\varepsilon_m k_{a,1}\left(1+A_1 s^{\beta_1}\right)C_{NP}-\rho_b k_{d,1} s_1 \tag{3}$$

and s_2 is the concentration of deposited particles due to straining and given by the phenomenological model (Bradford et al., 2003)

$$\frac{\partial\left(\rho_b s_2\right)}{\partial t}=\varepsilon_m k_{a,2}\left(1+x/d_{50}\right)^{-\beta_2}C_{NP}-\rho_b k_{d,2} s_2 \tag{4}$$

To calculate the changes caused by particle deposition on the macroscopic properties of the porous medium, namely the porosity, ε_m, the specific surface area, a, and permeability, k, the following relationships are used (Tosco and Sethi, 2010; Tosco et al 2014).

$$\varepsilon_m=\varepsilon_0-\varepsilon_{im}=\varepsilon_0-\frac{\rho_b}{\rho_s}s \qquad a(s)=a_0+a_p\theta\left(\frac{\rho_b}{\rho_p}\right)s \qquad k(s)=k_0\left(\frac{\varepsilon_m}{\varepsilon_0}\right)^3\left(\frac{a_0}{a}\right)^2 \tag{5}$$

where ε_0 is the initial porosity, ε_{im} is the fraction of initial porosity occupied by deposited particles, ρ_s is the density of particles deposit, a_p, is the specific surface area of nanoparticles, a_0 is the initial specific surface area of the porous medium, k_0 is the initial

absolute permeability of the porous medium, and θ is a parameter controlling the contribution fraction of deposited particles to the increase of the surface area a. Finally, the pressure gradient across the porous medium is given by Darcy law, which is written

$$\frac{\partial P}{\partial x} = -\frac{\mu}{k} u_d \tag{6}$$

where P is the fluid pressure, and μ is the viscosity of aqueous suspension.
Assuming that the porosity is fully occupied by deposited nanoparticles, the maximum concentration, s_{max}, and dimensionless concentration, s^*, are defined by

$$s_{max} = \rho_s \varepsilon_0 / \rho_b \qquad s^* = s / s_{max} \tag{7}$$

In addition, the following dimensionless variables are defined

$$P^* = P/P_0 \,, C_{NP}^* = C_{NP}/C_{NP0} \,, \; s_{1,2}^* = s_{1,2}/s_{max} \,, \xi = x/L, \tau = t u_d / \left(L\varepsilon_0\right), k^* = k/k_0 \tag{8}$$

where P_0 is the outlet (atmospheric) pressure, and C_{NP0} is the nZVI concentration in the feed suspension. By replacing Eqs.(7-8) into Eqs.(1)-(6), and after some manipulation we get the following dimensionless equations

$$\frac{\partial C_{NP}^*}{\partial \tau} = \frac{1}{1-s^*}\left(C_{NP}^* - \frac{\rho_s}{C_{NP0}}\right)\left(\frac{\partial s_1^*}{\partial \tau} + \frac{\partial s_2^*}{\partial \tau}\right) - \left(\frac{1}{1-s^*}\right)\frac{\partial C_{NP}^*}{\partial \xi} + \frac{\varepsilon_0}{Pe_{NP}}\left[\frac{\partial^2 C_{NP}^*}{\partial \xi^2} - \left(\frac{1}{1-s^*}\right)\frac{\partial C_{NP}^*}{\partial \xi}\frac{\partial s^*}{\partial \xi}\right] \tag{9}$$

$$\frac{\partial s_1^*}{\partial \tau} = \left(\frac{\varepsilon_0 C_0}{\rho_s}\right) D_{a,1}\left(1-s^*\right)\left[1 + A_1\left(s^* s_{max}\right)^{\beta_1}\right] C_{NP}^* - \varepsilon_0 Da_{d,1} s_1^* \tag{10}$$

$$\frac{\partial s_2^*}{\partial \tau} = \left(\frac{\varepsilon_0 C_0}{\rho_s}\right) D_{a,2}\left(1-s^*\right)\left(1 + \frac{\xi L}{d_{50}}\right)^{\beta_2} C_{NP}^* - \varepsilon_0 Da_{d,2} s_2^* \tag{11}$$

$$\frac{\partial P^*}{\partial \xi} = -\frac{1}{k^*}\left(\frac{L\mu u_d}{P_0 k_0}\right) \qquad k^* = \left(1-s^*\right)^3 \Bigg/ \left[1 + \left(\frac{a_p \theta \rho_s \varepsilon_0}{\rho_p a_0}\right) s^*\right]^2 \tag{12}$$

In the foregoing equations, a set of dimensionless numbers are included: the Peclet number of NPs, Pe_{NP}, the Damköhler number of nanoparticle attachment / detachment ($i = a, d$), $Da_{i,j}$, the dimensionless flow velocity, λ, defined by

$$Pe_{NP} = u_d L / D_{L,NP} \qquad Da_{i,j} = k_{i,j} L / u_d \qquad \lambda = L\mu u_d / \left(P_0 k_0\right) \tag{13}$$

3.3 Model of NP transport and NAPL remediation in porous media

To model the 1-dimensional fate of trapped NAPL ganglia (PCE source zone) when injecting a nZVI suspension in a porous medium, the aforementioned mass balances of nanoparticles transport are combined with: (i) a mass balance for nZVI advection, dispersion, and reactions

$$\frac{\partial\left(\varepsilon_m S_w C_{nZVI}\right)}{\partial t} + \frac{\partial\left(\rho_b s_0\right)}{\partial t} = -\frac{\partial\left(u_d C_{nZVI}\right)}{\partial x} + \frac{\partial}{\partial x}\left(\varepsilon_m S_w D_{L,NP}\frac{\partial C_{nZVI}}{\partial x}\right) - \varepsilon_m S_w R_{1,nZVI} - \varepsilon_m R_{2,nZVI} \tag{14}$$

(ii) a mass balance for dissolved PCE advection, dispersion, dissolution, and reaction

$$\frac{\partial\left(\varepsilon_m S_w C_P\right)}{\partial t} = -\frac{\partial\left(u_d C_P\right)}{\partial x} + \frac{\partial}{\partial x}\left(\varepsilon_m S_w D_{L,P}\frac{\partial C_P}{\partial x}\right) + k_m\left(C_{sol} - C_P\right) - \varepsilon_m S_w R_{1,P} \quad (15)$$

In Eqs.(14) and (15), S_w is the water saturation, $R_{1,nZVI}$ is the volumetric rate of nZVI reaction with dissolved PCE, $R_{2,nZVI}$ is the volumetric rate of the direct reaction of nZVI with PCE ganglia (NAPL), C_{nZVI} is the concentration of nZVI, namely the concentration of NP that have not yet reacted, s_0 is the total concentration of nZVI deposited on sand grains, C_P, is the dissolved PCE concentration, $D_{L,P}$ is the dissolved PCE longitudinal dispersion coefficient, k_m is the lumped mass-transfer coefficient of PCE ganglia dissolution, C_{sol} is the PCE solubility in aqueous phase, and $R_{1,P}$ is the volumetric rate of dissolved PCE reaction with nZVI. We assume that the concentrations of nZVI deposited on sand grains through mechanisms 1 and 2, s_{01} and s_{02}, respectively, are governed by attachment and detachment rates analogous to Eqs.(3-4), with identical kinetic constants.
During the nZVI injection, the NAPL saturation, S_{nw} (S_{nw}=1-S_w), varies because of (a) the dissolution of NAPL ganglia in aqueous phase, and (b) direct reaction of nZVI with NAPL ganglia. Therefore, the mass balance is written

$$\frac{\partial\left(\rho_{nw}\varepsilon_m S_{nw}\right)}{\partial t} = -k_m\left(C_{sol} - C_P\right) - \varepsilon_m S_w R_{2,P} \quad (16)$$

where ρ_{nw} is the density of PCE, and $R_{2,P}$ is the volumetric rate of the direct reaction of NAPL ganglia with nZVI.
Darcy law is given by the relationship

$$\frac{\partial P}{\partial x} = -\frac{\mu}{k k_{rw}} u_d \quad (17)$$

where k_{rw} is the water relative permeability, expressed by a Corey type model of the form

$$k_{rw} = S_w^{\,m_w} \quad (18)$$

In general, experimental datasets are used (Miller et al., 1990) to correlate the Sherwood number, $Sh = k_m {d_{50}}^2 / D_{m,P}$ with the Schmidt number, $Sc = \mu / \left(\rho_w D_{m,P}\right)$ and Reynolds number, $Re = \left(d_{50}\rho_w u_d\right) / \left(\mu\varepsilon_m S_w\right)$ through the relationship

$$Sh = p_1 Re^{p2} Sc^{p_3} \quad (19)$$

The effective diffusivity of nanoparticles and dissolved PCE in partially water-saturated porous media might be approximated by

$$D_{eff,NP} = D_{BM} / \left(F I_R \varepsilon_m S_w\right) \qquad D_{eff,P} = D_{m,P} / \left(F I_R \varepsilon_m S_w\right) \quad (20)$$

where F, I_R are the electrical formation factor, and resistivity index, expressed by Archie laws (Sahimi, 1995)

$$F = \varepsilon_m^{\,-n_f} \qquad I_R = S_w^{\,-n_r} \quad (21)$$

and n_f, n_r are the cementation and saturation exponent, respectively. The dispersion coefficients for nanoparticles and dissolved PCE might be approximated (Sahimi, 1995) by

$$D_{L,NP} = D_{eff,NP} + a_L u_p / \left(S_w \varepsilon_m\right) \qquad D_{L,P} = D_{eff,P} + a_L u_p / \left(S_w \varepsilon_m\right) \quad (22)$$

The dynamics of the reaction of suspended nZVI with PCE dissolved in aqueous phase has been studied experimentally in batch reactors and approximated numerically with the statistical shrinking-core model (Tsakiroglou et al., 2017). At nanoparticle scale, as the reaction proceeds, a layer (shell) of porous product (e.g. FeOOH) is created around its non-reacted core, so that dissolved PCE may diffuse through it to react with unreacted nZVI upon the interface (core-shrinking model). The simulated results of the shrinking-core model can be fitted with conventional kinetic models providing the volumetric reaction rates of dissolved PCE and nZVI as functions of bulk concentrations, namely (Tsakiroglou et al., 2017)

$$R_{1,P} = \frac{dC_P}{dt} = \left(\frac{3C_{sol}C_{NP0}k_r}{\rho_p} \right) \frac{dC_P^*}{d\tau} = \left(\frac{3C_{sol}C_{NP0}k_r}{\rho_p \langle r_p \rangle^{m_s}} \right) C_P^{*\,n_s} C_{nZVI}^{*\,m_s} \tag{23a}$$

$$R_{1,nZVI} = \frac{dC_{nZVI}}{dt} = \left(\frac{3C_{sol}C_{NP0}k_r}{\rho_p} \right) \frac{dC_{nZVI}^*}{d\tau} = \alpha_r \left(\frac{3C_{sol}C_{NP0}k_r}{\rho_p \langle r_p \rangle^{m_s}} \right) C_P^{*\,n_s} C_{nZVI}^{*\,m_s} \tag{23b}$$

where $\langle r_p \rangle$ is the mean particle radius, k_r is the kinetic constant of the surface PCE/Fe^0 reaction occurring at the interface between the nZVI core and reacted shell. The exponents n_s and m_s (reaction orders) estimated by fitting Eqs.(23a,b) to the transient responses of the dimensionless concentrations of nZVI and PCE, obtained from the numerical solution of the statistical shrinking core model (Tsakiroglou et al., 2017). The ratio α_r is a normalization factor of the reaction stoichiometry (Tsakiroglou et al., 2017), defined by

$$\alpha_r = \left(C_{sol} MW_{Fe} \right) / \left(C_{NP0} MW_{PCE} \right) \tag{24}$$

where MW_{Fe}, MW_{PCE} are the molecular weights of iron and PCE, respectively.

As the iron nanoparticles are flowing around the trapped PCE ganglia, a fraction of NPs may be attached on PCE/water interfaces and react directly with PCE ganglia (Tsakiroglou et al., 2016). Assuming that the reaction rate is proportional to the local concentration of suspended nZVI and the total specific interfacial area, the reaction kinetics may be approximated by

$$R_{2,P} = \frac{dS_w}{dt} = -C_{NP0} k_{NAPL} \left(1 - S_w \right)^{2/3} C_{nZVI}^* \tag{25a}$$

$$R_{2,nZVI} = \frac{dC_{nZVI}}{dt} = \alpha_n C_{NP0} k_{NAPL} \left(1 - S_w \right)^{2/3} C_{nZVI}^* \tag{25b}$$

where k_{NAPL} is the kinetic constant of the direct PCE ganglia reaction with nZVI, and α_n is the normalization factor of reaction stoichiometry, defined by

$$\alpha_n = \frac{MW_{Fe}}{MW_{PCE}} \tag{26}$$

The dimensionless variables defined by

$$C_{nZVI}^* = C_{nZVI} / C_{NP0} \quad , \quad C_P^* = C_P / C_{sol} \tag{27}$$

along with the variables defined by Eqs.(7-8) are replaced in Eqs.(14)-(17) and after some manipulation, four dimensionless partial differential equations are obtained for

C^*_{nZVI}, C^*_P, S_w, P^*, where the following dimensionless numbers are included: the Peclet number for dissolved PCE, Pe_P, the Damköhler number for the reaction of dissolved pollutant with nanoparticles, Da_{dp}, the Damköhler number for the reaction of bulk NAPL with nanoparticles, Da_{NAPL}, the Damköhler number for the dissolution of NAPL ganglia, Da_m, defined by

$$Pe_P = \frac{u_d L}{D_{L,P}} \qquad Da_{dp} = \frac{k_r L}{u_d} \qquad Da_{NAPL} = \frac{k_{NAPL} L}{u_d} \qquad Da_m = \frac{C_{sol} k_m L}{\rho_{nw} u_d} \tag{28}$$

The aforementioned equations along with Eqs.(9)-(11) comprise a transport-remediation model that is supplemented by the appropriate initial and boundary conditions. For the numerical solution of the mathematical models, and parameter estimation the software Athena Visual Studio (Stewart and Caracotsios, 2008) was used.

RESULTS AND DISCUSSION

The NP transport model was used to match the iron concentration breakthrough curve measured at the outlet of the sand column during a NP flow test, and to estimate the kinetic parameters of NP attachment and detachment rates under clean bed conditions. By ignoring the direct reaction of nZVI with trapped NAPL ganglia, and without using any other adjustable parameter, we simulated the process of the trapped PCE (source zone) remediation in sand column by injecting 1 PV of DDW followed by 4 PVs of nZVI suspension (Fig.1). The discrepancy observed between simulated and measured PCE concentration in effluent (Fig.1a) might be attributed to the uncertainty associated with PCE solubility in distilled water (DDW) and aqueous solution of CMC, respectively. The parameters of NP transport model were estimated under clean bed conditions while the simulation was done in a sand column at residual PCE saturation, and the discrepancy observed between measured and simulated iron concentration breakthrough curves seems reasonable (Fig.1a). The predicted PCE remediation efficiency (~21%, S_{wf}=0.819) is lower than the experimentally measured one (~32%, S_{wf}=0.845) (Fig.1b). The discrepancy observed might be regarded reasonable in the light of the large number of non adjustable parameters included in the numerical simulations (Fig.1b). Among others, the underestimation of PCE remediation efficiency (Fig.1b) might be attributed to the model assumption that neglects the reactivity of nZVI deposited on sand grains. During the initial stages of nZVI delivery, the NP deposition by mechanism 1 prevails. However, respectable changes of porosity are expected to take place at later stages of nZVI delivery when the NP deposition is dominated by straining (Fig.1c). Regarding the axial profile of simulated concentrations and water saturation, at the end of nZVI injection (τ=4.3 PV), we observe that at the axial position where the nZVI concentration vanishes, the reaction of dissolved PCE with nZVI ceases, the concentration of dissolved PCE increases rapidly, and water saturation is stabilized close to its initial value (Fig.1d). This means that the remediation of bulk PCE occurs over a limited length of the porous medium, where the concentration of delivered nZVI is discernible (Fig.1d).

Two reaction pathways of PCE source zone remediation in aquifers were considered: (1) PCE dissolution and reaction with suspended nZVI in aqueous phase; (2) direct reaction of suspended nZVI with trapped ganglia of PCE. Sensitivity analysis revealed that: (i) the

overall NAPL remediation rate predicted by the 1st pathway is much higher than those predicted by the 2nd pathway or both the 1st and 2nd pathways; (ii) the flow velocity, particle size distribution, and NAPL solubility affect respectably the overall NAPL remediation rate. Furthermore, the numerical model could be extended to 3-dimensions, heterogeneous porous media that simulate the hydrogeology of real aquifers, and dechlorination kinetics of other NAPLs. Under such conditions, the simulator could be utilized as computational tool to design nZVI injection for the in situ remediation of aquifers heavily contaminated by chlorinated solvents (PCE, TCE, etc).

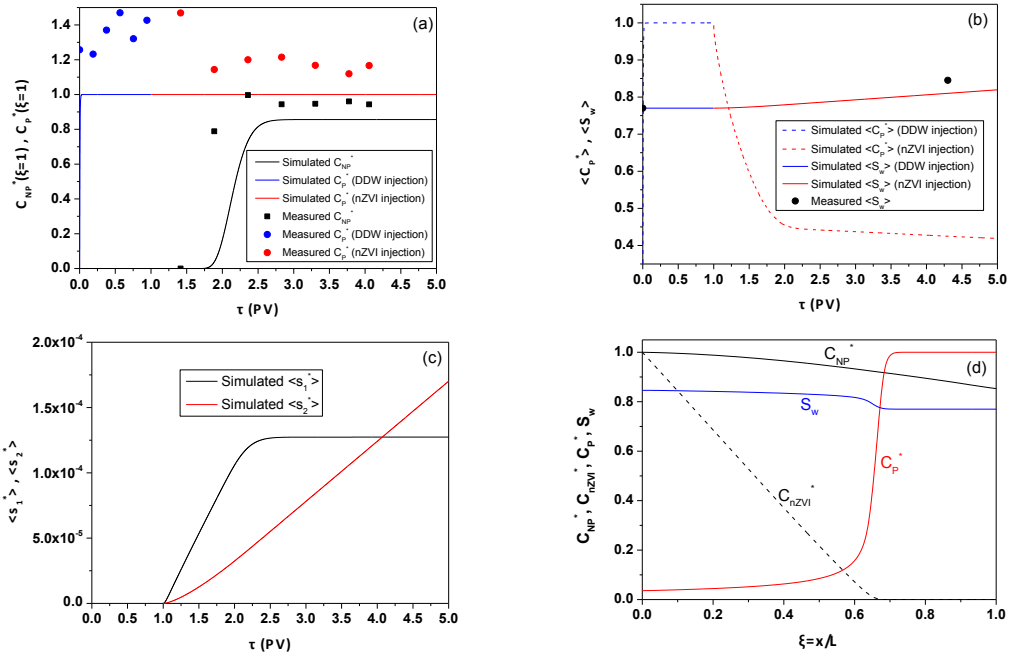

Figure 1. Simulation of the PCE source zone remediation in a sand column by injecting 1 PV of DDW and 3.3 PVs of nZVI suspension. (a) Measured vs simulated transient response of the iron and dissolved PCE concentrations in column effluent. (b) Simulated transient response of the column-averaged PCE concentration and water saturation. (c) Simulated transient responses of the column-averaged concentration of deposited nanoparticles. (d) Simulated axial profile of the concentration of NPs, nZVI, dissolved PCE and water saturation along the porous medium at the end of nZVI injection.

CONCLUSIONS

To design an efficient NAPL source zone remediation strategy, the parameter values must so be selected that the nZVI concentration is kept higher than zero over the longest length of the porous medium. The nanoparticles flow, and transport in porous media coupled with NAPL dissolution and reaction of nanoparticles with dissolved and bulk NAPL is a complicated problem and the numerical model developed here involves some simplifying assumptions. To improve the model predictability the following factors must be taken in account: (i) the gradual aggregation of nanoparticles and its effect on deposition rate and reaction kinetics; (ii) the reaction of nanoparticles deposited on sand grains with dissolved NAPL; (iii) the deposition rate of nanoparticles on NAPL ganglia and the kinetics of their direct reaction with them. However, in order to involve all foregoing processes in a continuum numerical model, well-designed experiments in

model porous media have to be combined with sophisticated approaches for the interpretation of experiments.

ACKNOWLEDGEMENTS

The research was co-financed by the European Union (European Social Fund-ESF) and Greek national funds in the context of the action "EXCELLENCE II" of the Operational Program "Education and Lifelong Learning" (project no 4118-SOILREM, "Optimizing the properties of nanofluids for the efficient in situ soil remediation").

REFERENCES

1. Babakhani, P., Bridge, J., Doong, R-A., Phenrat, T., 2017. Continuum-based models and concepts for the transport of nanoparticles in saturated porous media: a state-of-the-science review. *Adv. Colloid Interface Sci.* **246**, 75-104.
2. Bradford, S.A., Simunek, J., Bettahar, M., van Genuchten, M.T., Yates, S.R., 2009. Significance of straining in colloid deposition: Evidence and implications. *Water Resour. Res.* **42**, 12-25.
3. Bradford, S.A., Simunek, J., Bettahar, M., van Genuchten, M.T., Yates, S.R., 2003. Modeling colloid attachment, straining, and exclusion in saturated porous media. Env. Sci. Technol. 37, 2242-2250.
4. Fagerlund, F., Illangaserake, T.H., Phenrat, T., Kim, H.-J., Lowry, G.V., 2012. PCE dissolution and simultaneous dechlorination by nanoscale zero-valent iron particles in a DNAPL source zone. *J. Contam. Hydrol.* **131**, 9-28.
5. Miller, C.T., Poirier-Mcneill, M.M., Mayer, A.S., 1990. Dissolution of trapped nonaqueous phase liquids: mass-transfer characteristics. *Water Resour. Res.* **26**, 2783-2796.
6. Molnar, I.L., Johnson, W.P., Gerhard, J.I., Willson, C.S., O'Carroll, D.M., 2015. Predicting colloid transport through saturated porous media: a critical review. *Water Resour. Res.* **WR017318**, 6804-6845.
7. Mueller, N.C., Braun, J., Bruns, J., Cernik, M., Rissing, P., Rickerby, D., Nowack, B., 2012. Application of nanoscale zero valent iron (NZVI) for groundwater remediation in Europe. *Environ. Sci. Pollut. Res.* **19**, 550-558.
8. Sahimi, M., 1995. Flow and Transport in Porous Media and Fractured Rock. From Classical Models to Modern Approaches, VCH, NY.
9. Stewart, W.E., Caracotsios, M., 2008. Computer-Aided Modeling of Reactive Systems. John Wiley & Sons, Hoboken, New Jersey.
10. Taghavy, A., Costanza, J., Pennell, K.D., Abriola L.M., 2010. Effectiveness of nano-scale zero-valent iron for treatment of a PCE-DNAPL source zone. *J. Contam. Hydrol.* **118**, 128-142.
11. Tosco, T., Sethi, R., 2010. Transport of non-newtonian suspensions of highly concentrated micro- and nanoscale iron particles in porous media: A modeling approach. *Environ. Sci. Technol*. **44**, 9062–9068.

12. Tosco, T., Petrangeli Papini, M., Cruz Viggi, C., Sethi, R., 2014. Nanoscale zerovalent iron articles for groundwater remediation: a review. *J. Clean. Prod.* **77**, 10–21.
13. Tsakiroglou, C.D., Hajdu, K., Terzi, K., Aggelopoulos, C.A., Theodoropoulou, M.A., 2017. A statistical shrinking core model to estimate the overall dechlorination rate of PCE by an assemblage of zero-valent iron nanoparticles. *Chem. Eng. Sci.* **167**, 191-203.
14. Tsakiroglou, C.D., Terzi, K., Sikinioti-Lock, A., Hajdu, K., Aggelopoulos, C., 2016. Assessing the capacity of zero valent iron nanofluids to remediate NAPL-polluted porous media. *Sci. Total Environ.* **563–564**, 866–878.